Proceedings of the 17th World Congress
The International Federation of Automatic Control
Seoul, Korea, July 6-11, 2008

Nanomanipulation and Nanoassembly of Carbon Nanotubes Inside Electron Microscopes

Masahiro Nakajima*. Pou Liu.*
Toshio Fukuda*

** Department of Micro-Nano Systems Engineering, Nagoya University*
Furo-cho, Chikusa-ku, Aichi, Japan
(Tel: +81-52-789-2717; e-mail: nakajima@mein.nagoya-u.ac.jp).

Abstract: We report nanomanipulation and nanoassembly of carbon nanotubes (CNTs) through nanorobotic manipulation inside electron microscopes. A hybrid nanorobotic manipulation system, which is integrated with a nanorobotic manipulator inside a transmission electron microscope (TEM) and nanorobotic manipulators inside a scanning electron microscope (SEM), is used. The elasticity of a multi-walled CNT (MWNT) is measured inside a TEM. The telescoping MWNT is fabricated by peeling off outer layers through destructive fabrication process. The electrostatic actuation of telescoping MWNT is directly observed by a TEM. A cutting technique for CNTs assisted by the presence of oxygen gas is also presented. The cutting procedure was conducted in less than 1 minute using a low-energy electron beam inside a scanning electron microscope. A bending technique of a CNT assisted by the presence of oxygen gas is also applied for the 3-D fabrication of nanostructure. We expect that these techniques will be applied for the rapid prototyping nanoassembly of various CNT nanodevices.

1. INTRODUCTION

Nanomanipulation has been received much more attention, because it is an effective strategy for the property characterizations of individual nano-scale materials, and the construction of nano-scale devices. Scanning probe microscopes (SPMs), like scanning tunnelling microscopes (STMs) or atomic force microscopes (AFMs), have functions of both observation and manipulation. Their high resolution makes them capable of atomic manipulation (Eigler *et al.*, 1990; Hertel *et al.*, 1998). However their observation space is too narrow and constrained in a 2-D plane. On the other hand, electron microscopes, such as scanning electron microscopes (SEMs) and transmission electron microscopes (TEMs), show their uniqueness on the capability to contain an independent nanomanipulator. TEMs have high enough resolutions for nanomanipulation, and some groups have demonstrated nanomanipulation using a piezo-tube driven nanomanipulator inside the specimen holder (Cummings *et al.*, 2000; Kizuka *et al.*, 1997). The issue of the TEM nanomanipulator is that its specimen chamber and observation area are too narrow to contain manipulators with complex functions. Here we propose an exchangeable robotic manipulator between a SEM and a TEM (Nakajima *et al.*, 2004; Nakajima *et al.*, 2006). The strategy is named as hybrid nanomanipulation so as to differentiate it from those with only an exchangeable specimen holder. The most important feature of the manipulator is that it contains several passive DOFs, which makes it possible to perform relatively complex manipulations whereas to keep compact volume to be installed inside the narrow vacuum chamber of a TEM.

As a typical nanomaterial, carbon nanotubes (CNTs) have been widely investigated to show their extraordinarily mechanical, electronic and chemical properties. The nanotubes have been proposed as a basic building block for the next generation of nano-electronic and mechanical systems (Dai *et al.*, 1996; Kim *et al.*, 1999). Their lengths are one of important parameters for the fabrication and assembly of nanodevices based on CNTs. A number of cutting techniques of CNTs have been proposed previously (Suzuki *et al.*, 2004; Yuzvinsky *et al.*, 2005). We propose a technique for high-speed cutting of CNTs inside a SEM by introducing oxygen gas into the vicinity of the samples (Liu *et al.*, 2006). The presence of oxygen gas can be readily used for the bending of CNT by controlling the irradiation of electron beam. The 3-D nanostructure is assembled using a CNT with the cutting and bending techniques (Liu *et al.*, 2006).

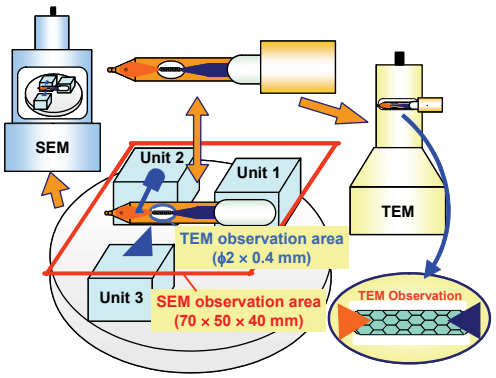

Fig 1. A schematic of Hybrid Nanorobotic Manipualtion System.

2. HYBRID NANOROBOTIC MANIPULATION SYSTEM INSIDE SCANNING AND TRANSMISSION ELECTRONMICROSCOPES

Table1. Specification of Hybrid Nanorobotic Manipulation System

Items	Specifications
TEM Nanorobotic Manipulator (Fig. 2, Fig. 3)	
DOFs	3 DOFs (X, Y, Z), Passive 3 DOFs (X, Y, Z)
Actuators	4 multi-layer piezoelectric devices
Work. Space	~ 8 μm × ~ 60 μm × ~ 60 μm
SEM Nanorobotic Manipulator (Fig. 2)	
DOFs	Unit1: 2 DOFs (X, Y), Unit2: 3 DOFs (X, Y, Z), Unit3: 3 DOFs (X, Y, Z), Total: 8 DOFs
Actuators	6 Picomotors™, (Unit1, Unit2,Uni3-Z) 2 Nanomotors™ (Unit3-X,Y)
Work. Space	~ 16 mm × ~ 16 mm × ~12 mm
Positioning Resolution	~ 30 nm (Unit 1, Unit2, Unit3: Z), ~2nm (Unit3: X, Y)
TEM (H-800, Hitachi)	
Acc. Volt.	35 ~ 200 kV
Resolution	0.204 nm(lattice-lattice), 0.45 nm (point-point)
Obs. Space	ϕ 2 mm × ± 0.3 mm
TEM (JEM-2100, JEOL)	
Acc. Volt.	80 ~ 200 kV
Resolution	0.14 nm(lattice-lattice)
Obs. Space	ϕ 2 mm × 0.4 mm
FE-SEM (JSM-6500F, JEOL)	
Acc. Volt.	0.5 ~ 30 kV
Resolution	1.5 nm (at Acc. Volt.: 15 kV)
Obs. Space	70 mm × 50 mm × 40 mm

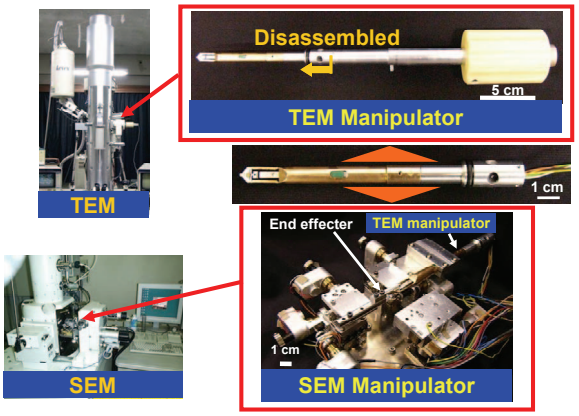

Fig. 2. Overview of constructed hybrid nanorobotic manipulation system.

We propose a hybrid nanorobotic manipulation system which is integrated a TEM nanorobotic manipulator (TEM manipulator) and a SEM nanorobotic manipulator (SEM manipulator) (Nakajima *et al.*, 2004; Nakajima *et al.*, 2006). Figure 1 shows a schematic of the hybrid nanorobotic manipulation system. A TEM nanomanipulator can be used inside a SEM and a TEM, and be driven with SEM nanomanipulators for the setting of TEM samples. This system realizes an effective sample preparation inside a SEM with wide enough working area and degrees of freedom (DOFs) of manipulation, and a high resolution measurement and evaluation of samples inside a TEM. Figure 2 shows the overview of the constructed hybrid nanorobotic manipulation system. Table 1 is a detailed list of the hybrid nanorobotic manipulation system specifications.

3. *IN SITU* MEASUREMENT OF ELASTICITY OF CARBON NANOTUBES INSIDE TRANSMISSION ELECTRON MICROSCOPE

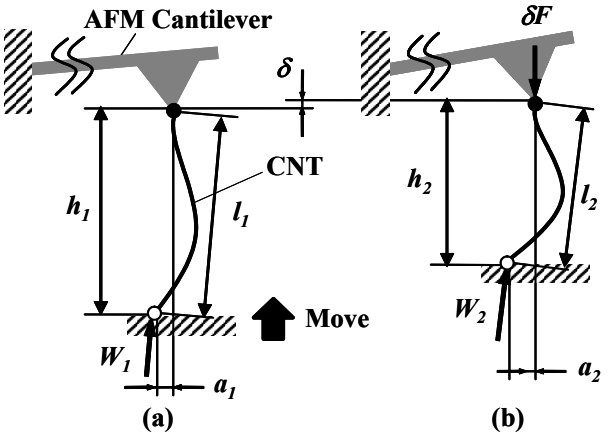

Fig. 3. Schematic diagram of buckling a carbon nanotube for measurement of its bending modulus.

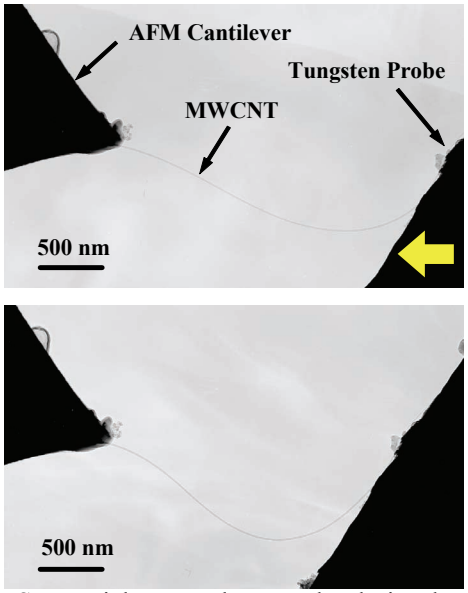

Fig. 4. Sequential TEM photographs during buckling a multi-walled carbon nanotube.

The elasticity of multi-walled CNTs (MWNTs) are measured inside a TEM with *in situ* force measurement using an AFM cantilever. By the TEM observation, the precise measurement of the diameter of CNTs, included their inner cores, are determined for the precise mechanical measurements. Figure 3 shows the analytic model for the measurement by buckling process. The elastic modulus of a CNT E_{CNT} is calculated from the following equation,

$$E_{CNT} = \frac{64k\delta}{(d_{oCNT}{}^4 - d_{iCNT}{}^4)\pi^3(h_2/(c\,l_2)^3 - h_1/(c\,l_1)^3)} \qquad (1)$$

where, k is the spring constant of an AFM cantilever (Olympus OMCL-TR400PB, k: 0.03 N/m), δ is the deflection of an AFM cantilever, d_{oCNT} and d_{iCNT} are outer and inner diameter of the CNT, and c is a constant to calculate the effective length (c: 0.8). Figure 4 shows two sequential TEM photographs during buckling a MWNT (d_{oCNT}: 14.3 nm, d_{iCNT}: 3.2 nm, produced by arc-discharge method (Saito *et al.*, 1993). One end of a CNT is fixed on an AFM cantilever by Electron-Beam-Induced Deposition (EBID). The other end is adhered to a tungsten needle probe by van der Waals forces.

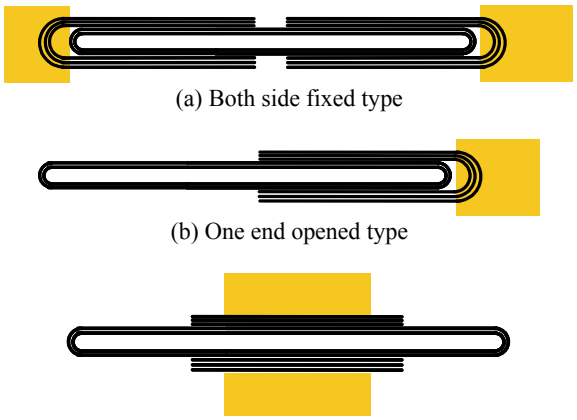

(a) Both side fixed type

(b) One end opened type

(c) Both end opened type

Fig. 5. Schematic diagram of telescoping nanotubes.

From these images, the parameters are measured as a_1: 0.447 μm, a_2: 0.318 μm, h_1: 2.36 μm, and h_2: 2.10 μm. The values of l_1, l_2, and δ are calculated as 2.41 μm, 2.12 μm, and 84.0 nm. Hence the elastic modulus of this CNT E_{CNT} is calculated to be 1.23 TPa.

4. *IN SITU* FABRICATION AND ACTUATION OF TELESCOPING NANOTUBES INSIDE TRANSMISSION ELECTRON MICROSCOPE

4.1 Fabrication of Telescoping Nanotubes

The telescoping carbon nanotube, which is fabricated by peeling off its outer layers, is one of the most interesting nanostructures (Fig.5). In this work, we fabricate the telescoping structure by peeling off its outer layers of a MWNT through destructive fabrication process.

Single MWNT is picked up on the tungsten probe, which is etched by forces-ion-beam (FIB), inside a SEM by EBID technique. The MWNTs are synthesized by arc discharge method (Saito *et al.*, 1993). One end of MWNT is freed, and the other end is fixed by EBID. This probe is fixed on the passively driven TEM sample stage. Another tungsten probe etched by FIB is fixed on the TEM manipulator as an anode. The MWNT is set the position using TEM sample stage driven by SEM manipulator within the working area of TEM manipulator. Then the free end is also fixed on the tungsten probe fixed TEM manipulator by EBID inside a TEM by controlling its spot size as ~100 nm. After both side fixations, the tungsten probe fixed on TEM manipulator is moved and tensile stress is applied on MWNT. When the tensile stress is reached at fracture stress, the outer layers of MWNT are destructed and inner core is pulled out. We called this process as destructive fabrication process.

Figure 6 shows sequential TEM images of the destructive fabrication process. Fig. 6 (a) shows one end freed carbon nanotube which is picked up inside SEM on tungsten probe. The external diameter is ~28 nm and internal diameter is ~2 nm from TEM image. The other free end is fixed on the tungsten probe of the TEM manipulator by EBID inside TEM and then moving the one end stage (Fig. 6 (b)). Its outer layers are destroyed by tensile stress and the inner core is

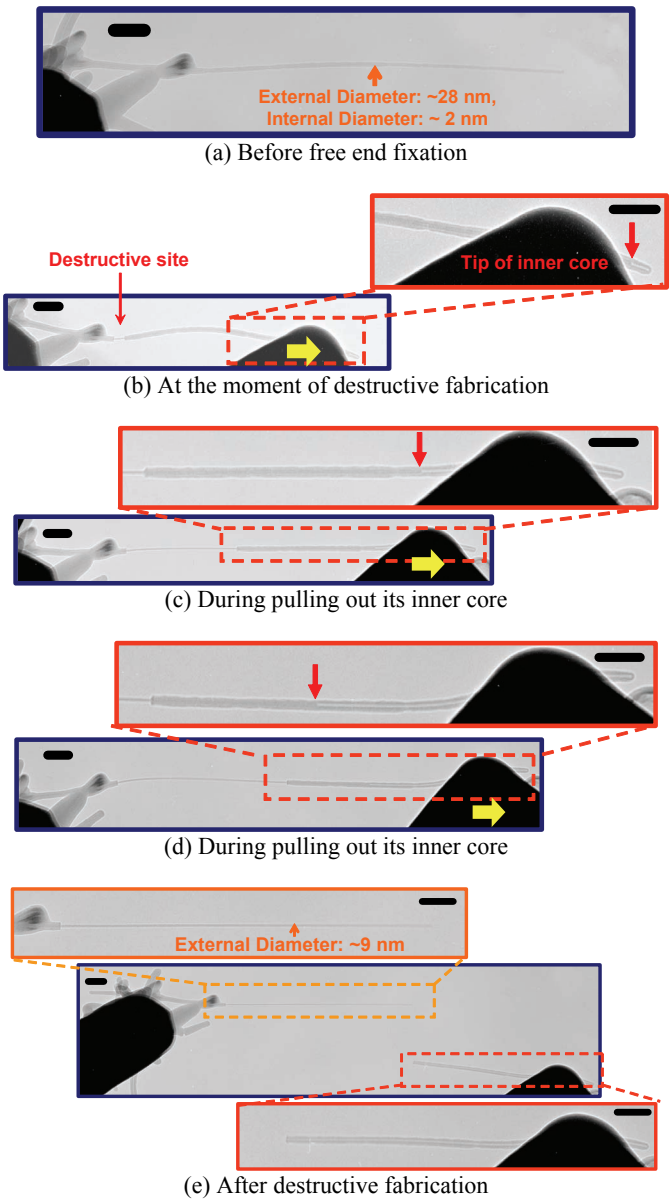

(a) Before free end fixation

(b) At the moment of destructive fabrication

(c) During pulling out its inner core

(d) During pulling out its inner core

(e) After destructive fabrication

Fig. 6. Sequential TEM images of destructive fabrication of multi-walled carbon nanotube (Scale bar: 100 nm).

pulled out (Fig. 6 (b)). As shown in Fig. 6 (c) and Fig. 6 (d), the inner core is smoothly pulled out. Fig. 6 (e) shows the inner core pulled out completely. The external diameter of the fabricated inner core is ~9 nm. From these in-situ experiments, we confirmed that the carbon nanotube is certainly peeled off its outer layers.

4.2 Nanoactuation of Telescoping Nanotube by applying Electrostatic Fields

The electrostatic actuation of telescoping MWNT is directly observed inside a TEM. In this work, one-end opened MWNT is used for one directional actuation. The schematic diagram of experimental setup is as shown in Fig. 7. The other end is fixed on the substrate by EBID technique. The telescoping structure is set against another probe as an anode inside a TEM by the nanomanipulator. Electrostatic force F_E

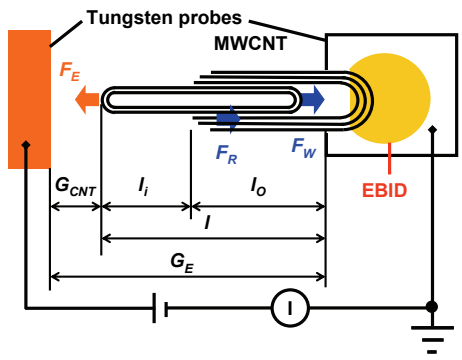

Fig. 7. Schematic diagram of electrostatic actuation of telescoping MWNT

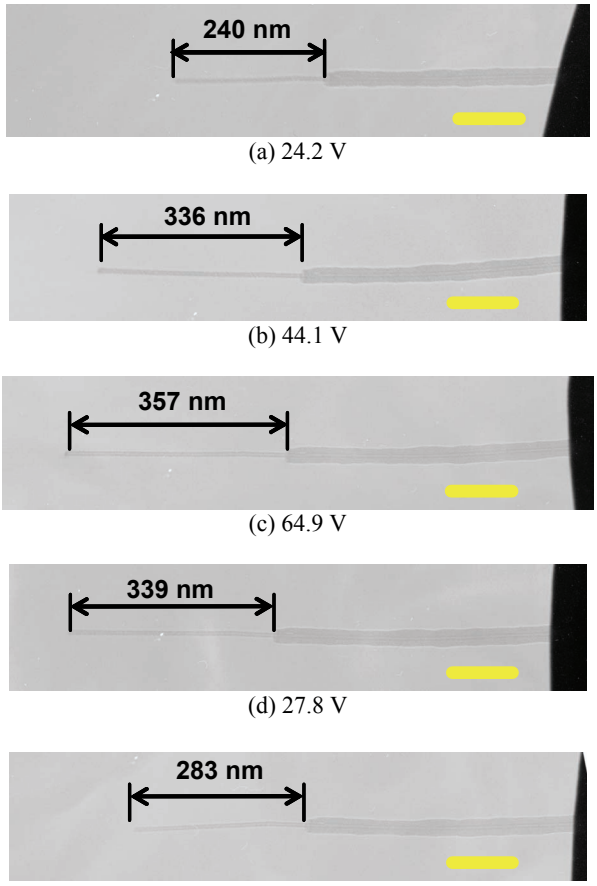

Fig. 8. Actuation of telescoping MWNT at each applied voltage. (Scale bar: 100 nm)

is generated at the tip of an inner core by applied bias voltage. The circuit current is measured to detect the field emission current from telescoping structure. On increasing the applied voltage, the inner core is actuated by the electrostatic force F_E in its axial direction. The sliding resistance force F_R and van der Waals force F_W are worked on the inner core. The sliding resistance force F_R is quite low, and it is lower than van der Waals forces F_W from the experimental results. Hence, when the electrostatic force F_E is removed, the inner core can be automatically retracted inside outer layers by van der Waals forces F_W.

Telescoping structure is destructively fabricated inside a TEM. The outer layers are fabricated as ~6.6 nm from ~8.4 nm. After positioning against the anode on TEM manipulator, DC bias voltage is applied. The distance between tungsten probes G_E is fixed at ~1.2 μm. Figure 8 shows the sequence TEM images at each applied voltage. It is clearly observed that the length of inner core l_i is extended and retracted depend on the applied voltage. The length of outer layers l_o is also increased and decreased by applied voltage. On increasing the applied voltage, the telescoping MWNT is deflected on the concentrated electric field. The generated electric field is vertical on the substrate. Hence, initially bent MWNT is vertically stood on the substrate. This is caused for the change of outer layers length l_o. The initial bending angles of telescoping MWNT are obtained ~30 ° in an observation plane from TEM image and ~40 ° in a perpendicular observation plane calculated from maximum and minimum l_o.

On increasing the applied voltage, the inner core is insensitive at higher than ~45 V. The maximum extended inner core length is ~179 nm at ~65V (Initial l_i: ~178 nm, maximum l_i: ~357 nm). On decreasing the applied voltage, the inner core is not fully retracted; it has approximately ~105 nm hysteresis (Final l_i: ~283 nm). The hysteresis might be caused by its bending. The retraction is caused by van der Waals forces; it is given by following equation (Cummings *et al.*, 2000),

$$F_W = 0.16C = 0.32\pi r_i \qquad (2)$$

where, C is the circumference of inner core of telescoping MWNT and r_i is its radius. This equation means the van der Waals force is independent on the contact area between inner core and outer layers. In this case, van der Waals force F_W is calculated as ~3 nN (C: ~20.7 nm, r_i: ~3.3 nm).

5. ASSEMBLY OF 3-D NANOSTRUCTURES BY IRRADIATION BY ION AND ELECTRON BEAMS

5.1 Defects insertion in Carbon Nanotubes by Gallium Ion beam

Defect is one of the important parameters for the properties of nanomaterials. By inserting the defects on the crystallized materials, their shapes are dramatically changes. We use the Focused-Ion-Beam (FIB, SII SMI-2050) for inserting the defects inside CNTs to change their structural shapes. In this experiment, the multi-walled carbon nanotubes with 20~50 nm diameters were synthesized by the standard arc-discharge method (Saito et al., 1993). The High-Resolution TEM (HR-TEM) image of raw CNTs is shown in Fig. 9. The fine layered structures are clearly shown. The TEM images of the CNTs irradiated by ion beam are shown in Fig. 10. Fig. 10 (a) – (c) shows CNTs irradiated at different dose rates: 5.0, 0.5, 0.1 × 10^{-15} ions/cm^{-2}. By increasing the dose rate of ion beam, the defects are readily inserted for bending their shapes (Fig. 10 (a)). By irradiating on the middle beam condition, the shapes are kept however the crystallized layers are changes as amorphous structures (amorphous-CNT) (Fig. 10 (b)). By irradiating on the relatively low beam condition, the

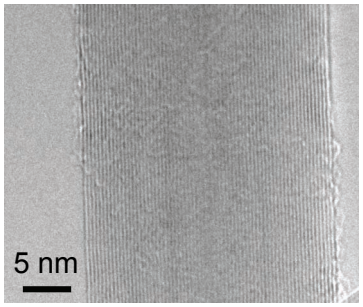

Fig. 9 HR TEM image of raw MWNTs.

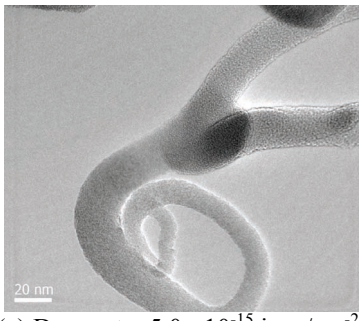

(a) Dose rate: 5.0×10^{-15} ions/cm^{-2}.

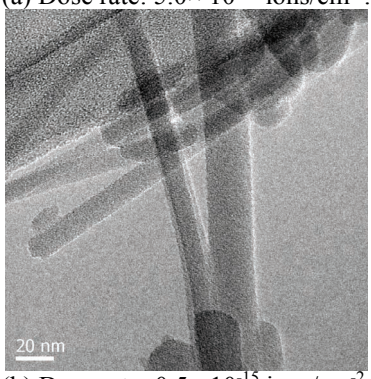

(b) Dose rate: 0.5×10^{-15} ions/cm^{-2}.

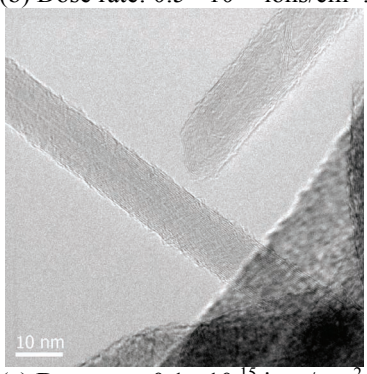

(c) Dose rate: 0.1×10^{-15} ions/cm^{-2}.

Fig.10 Irradiation of focused ion beam on raw MWNTs.

outer layers are slightly attacked, however the fine layers structures are maintained in inner parts (Fig. 10 (c)).

5.2 Cutting of Carbon Nanotube by Oxygen Gas

We show the cutting of a single CNT at high speed in the presence of oxygen and with the gas nozzle at 90 μm from the samples. We fixed a bundle of CNTs on a stage using electrically conductive tape. Oxygen gas (purity of 99.99995 %) was introduced into the vicinity of the sample through a glass nozzle with a 20 μm opening at the end, and

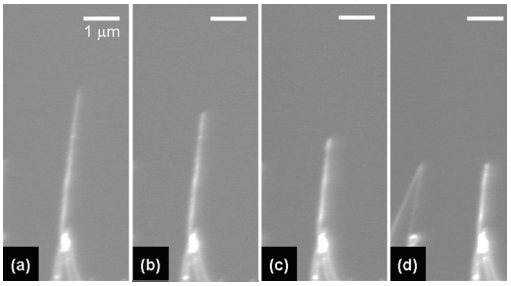

Fig. 11. (a) Before and (b-d) after cutting of a single CNT in less than 1 minute.

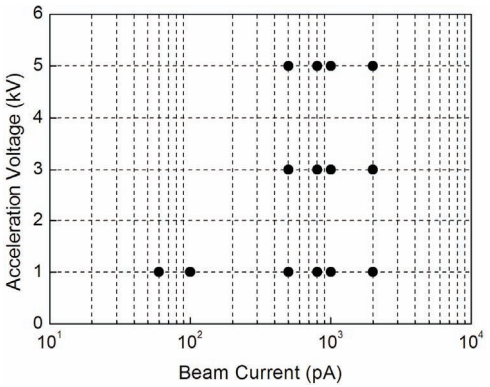

Fig. 12. Cutting of CNTs in less than 1 minute under various acceleration voltages and beam currents show by the black circles.

was regulated by a digital mass flow controller. The CNTs were observed using an acceleration voltage of 5 kV and cut normally using 1 kV inside the SEM. We selected the spot mode of the electron beam to cut the CNTs. The vacuum in the specimen chamber was reduced from 10^{-4} to 10^{-2} Pa when oxygen gas was introduced at 1 sccm.

A single CNT was cut by the electron beam in the presence of oxygen gas. Cutting was performed using the same electron beam current, acceleration voltage as the two previous cases. The vacuum pressure was 1.6×10^{-2} Pa and the oxygen gas flow rate conditions were the same as previously, however, the nozzle was located at a distance of 90 μm from the CNT in this case. Figure 11(a) shows the CNT before cutting, Fig. 11(b) shows the CNT after a length of 650 nm has been cut off and Fig. 11(c) shows the CNT after removing a further 700 nm. Figure 11(d) shows the cutting of a CNT such that it has the same length as the one on the left. These experimental results demonstrate that the length of CNT can be precisely controlled by cutting using an electron beam, assisted with oxygen gas. The acceleration voltages and the beam currents that can cut CNTs in less than 1 minute are shown in Fig. 11. Cutting is easy and rapid at low-acceleration voltages and high beam currents. The presence of oxygen gas in the vicinity of the CNT can be used also for the bending technique.

5.3 3-D Assembly of Carbon Nanotube

A 3-D nanostructure is constructed by the electron-beam-induced nanofabrication. The assembly progress of the structure is shown step by step in Figure 13. Figure 13 (a) shows a CNT picked up by an AFM cantilever and

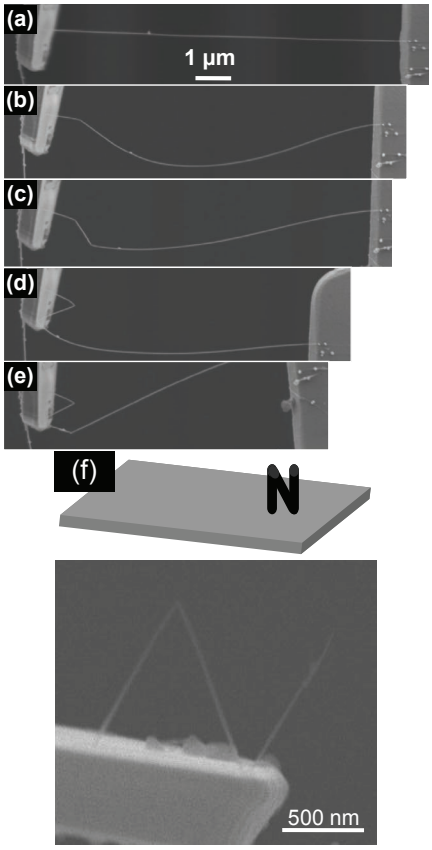

Fig. 13. Assembly of 3-D nanostructure based on a CNT assisted with fixing (a), bending (b)-(d), and cutting (e) techniques. The letter N stands on the substrate (f).

manipulated by the nanorobotic manipulator. The other end of the CNT was fixed on AFM cantilever surface by a tungsten deposit, produced by the EBID technique. The other end was set to touch the surface of another AFM cantilever. The bending technique irradiating by the electron beam was applied on the CNT and, as can be seen from Figure 13 (b), the CNT was bent at this point. The direction and angle of bending can be controlled by the manipulator. The first bending was followed by another bend in other CNT point, as shown in Figure 13 (c). The location and orientation of the CNT was changed by the manipulator and the second knick was set to touch the substrate as shown in Figure 13 (d). Finally, the CNT was cut at third point shown in Figure 13 (e) and the created 3-D nanostructure was separated from the substrate one. As the result, a letter "*N*" was assembled in a CNT and stand on the substrate at two points as shown in Figure 13 (f). The two points attach the structure on the substrate only by van der Waals force.

6. CONCLUSIONS

A hybrid nanorobotic manipulation system, which is integrated with a nanorobotic manipulator inside a TEM and a SEM, has been presented. The electrostatic actuation of telescoping MWNT was directly observed inside a TEM. The telescoping MWNT was fabricated by peeling off outer layers through destructive fabrication process. A cutting technique for CNTs assisted by the presence of oxygen gas has been also presented. The cutting procedure was conducted in less than 1 minute using a low-energy electron beam inside a scanning electron microscope. A bending technique of a CNT assisted by the presence of oxygen gas was applied for the 3-D fabrication of nanosturucture.

ACKNOWLEDGMENTS

The authors are grateful to Prof. Y. Saito at Nagoya University for providing us with MWNTs. This work was partially supported by MEXT KAKENHI.

REFERENCES

Cumings J., and A. Zettl, (2000). Low-Friction Nanoscale Linear Bearing Realized from Multiwall Carbon Nanotubes, *Science*, **289**, 602-604.

Dai H., J. H. Hafner, A. G. Rinzler, D. T. Colbert, and R. E. Smalley, (1996). Nanotubes as nanoprobes in scanning probe microscopy, *Nature*, **384**, 147-150.

Dong L. X., F. Arai, and T. Fukuda, (2001). 3D nanorobotic manipulations of multi-walled carbon nanotubes, *Proc. of the 2001 IEEE Int. Conf. on Robotics and Automation (ICRA2001)*, 632-637.

Eigler D. M., and E. K. Schweizer, (1990). Positioning single atoms with a scanning electron microscope, *Nature*, **344**, 524-526.

Hertel T., R. Martel, and P. Avouris, (1998). Manipulation of individual carbon nanotubes and their interaction with surfaces, *J. Phys. Chem*. B, **102**, 910-915.

Kim P., and C. M. Lieber, (1999). Nanotube Nanotweezers, *Science*, **286**, 2148-2150.

Kizuka T., K. Yamada, S. Deguchi, M. Naruse, and N. Tanaka, (1997). Cross-sectional time resolved high-resolution transmission electron microscopy of atomic-scal contact and noncontact-type scannins on gold surfaces, *Phys. Rev. B*, **55**, 7398-7401.

Nakajima M., F. Arai, L. X. Dong, and T. Fukuda, (2004). Hybrid Nanorobotic System inside Scanning Electron Microscope and Transmission Electron Microscope,

Nakajima M., F. Arai, and T. Fukuda, (2006). In situ Measurement of Young's Modulus of Carbon Nanotube inside TEM through Hybrid Nanorobotic Manipulation System, *IEEE Trans. Nanotech.*, **5**, 243-248.

Liu P., F. Arai, and T. Fukuda, (2006). Cutting of Carbon Nanotubes Assisted with Oxygen Gas inside a Scanning Electron Microscope, *Appl. Phys. Lett.*, **89**, 113104.

Liu P., K. Kantola, T. Fukuda, and F. Arai, (2007). Cutting of Carbon Nanotubes Assisted with Oxygen Gas inside a Scanning Electron Microscope, *Proc. of IEEE Int. Conf. on Robotics and Automation (ICRA2007)*, 441-446.

Saito Y., T. Yoshikawa, and M. Inagaki, (1993). Growth and structure of graphitic tubules and polyhedral particles in arc-discharge, *Chem. Phys. Lett.*, **204**, 277-282.

Suzuki S., K. Kanzaki, Y. Homma, and S. Fukuba, (2004). Low-Acceleration-Voltage Electron Irradiation Damage in Single-Walled Carbon Nanotubes, *Jpn. J. Appl. Phys.*, **43**, L1118.

Yuzvinsky T. D., A. M. Fennimore, W. Mickelson, C. Esquivias, and A. Zettl, (2005). Precision cutting of nanotubes with a low-energy electron beam, *Appl. Phys. Lett.*, **86**, 053109.